Density-Functional Computation of ^{99}Ru NMR Parameters

Michael Bühl,*[a, c] Sander Gaemers,[b] and Cornelis J. Elsevier[b]

Dedicated to Professor Dr. Paul von Ragué Schleyer on the occasion of his 70th birthday

Abstract: Gradient-corrected and hybrid variants of density-functional theory are used to compute the geometries and ^{99}Ru chemical shifts of RuO_4, $[RuCp_2]$, $[K_4Ru(CN)_6]$, $[Ru_3(CO)_{12}]$, $[Ru(CO)_3X_3]^-$ (X = Cl, I), $[Ru(CO)_2Cl_4]^{2-}$, $[Ru(bipy)_3]^{2+}$, and $[Ru(CO)_2(i\text{Pr-DAB})(X)(Y)]$ [XY = Cl_2, I_2, MeCl, MeI, or $(SnMe_3)_2$]. For this set of compounds, substituent effects on $\delta(^{99}Ru)$ are somewhat underestimated with the BPW91 pure density functional but are described well by the B3LYP hybrid functional, which can also be used to reproduce empirical trends in electric field gradients (EFGs) at the Ru nucleus qualitatively. In the $[Ru(CO)_2(i\text{Pr-DAB})XY]$ series, trends in the computed EFGs parallel those in the observed ^{99}Ru NMR linewidths, in accordance with the quadrupolar relaxation mechanism expected for this nucleus. For this series of compounds, the use of X-ray-derived geometries affords a worse correlation between calculated EFGs and experimental linewidths than does the use of optimized geometries.

Keywords: density functional calculations · electric field gradients · NMR spectroscopy · quadrupolar relaxation · ruthenium

Introduction

Nuclear magnetic resonance spectroscopy of heteronuclei, particularly transition-metal NMR for probing structure and reactivity of organometallic and coordination compounds, has gained substantial importance for chemists over the last decades.[1, 2] A number of metals have not yet been observed by NMR. For other metals, few NMR data have been obtained so far, which is mainly because of their low gyromagnetic ratio combined with low isotopic abundance and/or their quadrupole character. Yet, in view of the rich chemistry involving such metals, investigations concerning such nuclei are required in order to establish, for example, structure – shift – activity relations.[2] In this respect ^{99}Ru NMR is of considerable interest. Relatively few data have been accumulated for this nucleus and the chemical shifts and linewidths observed have not been the subject of systematic studies involving computational methods.

In view of the huge spectrum of methods theoreticians can offer to the chemist for numerical applications,[3] the importance of carefully validating any particular approach cannot be overemphasized. This holds especially true in the booming field of density-functional theory (DFT), where success and failure are hard to estimate beforehand. Transition-metal NMR chemical shifts are a case in point: Even though DFT is now well established as a reliable tool for the computation of geometries, energetics,[4] and NMR properties[5] of transition metal complexes, the chemical shifts of the metal nuclei themselves remain a challenge. This is because the results can be very sensitive to the particular density functional employed. In the cases studied hitherto, hybrid functionals such as the popular B3LYP combination have proven to be superior to "pure" density functionals, in particular for ^{57}Fe,[6] ^{103}Rh,[6] and ^{59}Co[7] chemical shifts, as well as for $\delta(^{51}V)$ values.[8] For ^{95}Mo chemical shifts, on the other hand, the opposite has been found, and B3LYP has yielded spectacular errors in special cases.[5b, 9] In order to gain more experience concerning the performance of these DFT methods, we carried out a systematic study of DFT-derived ^{99}Ru chemical shifts, the results of which we present here.

Apart from these technical aspects, motivation for a theoretical study of this long-neglected nucleus arises from the fact that its observation is fairly straightforward with modern NMR techniques. In a single recent study, some of us have approximately doubled the number of recorded ^{99}Ru NMR spectra[10] and have demonstrated that ^{99}Ru NMR spectroscopy can be a valuable tool for analytical purposes, as

[a] Dr. M. Bühl
Organisch-chemisches Institut
Universität Zürich, Winterthurerstr. 190
8057 Zürich (Switzerland)
E-mail: buehl@mpi-muelheim.mpg.de

[b] Dipl.-Chem. S. Gaemers, Prof. Dr. C. J. Elsevier
Institute of Molecular Chemistry
Universiteit van Amsterdam, Nieuwe Achtergracht 166
1018 WV Amsterdam (The Netherlands)

[c] Dr. M. Bühl
Present address:
Max-Planck-Institut für Kohlenforschung
Kaiser-Wilhelm-Platz 1, 45470 Mülheim an der Ruhr (Germany)
Fax: (+49) 208-306-2996

Supporting information for this article is available on the WWW under http://www.wiley-vch.de/home/chemistry or from the author.

 © WILEY-VCH Verlag GmbH, D-69451 Weinheim, 2000 0947-6539/00/0617-3272 $ 17.50+.50/0

well as for probing steric and electronic effects exerted by the ligands.

Like the chemical shifts, the linewidths of the ^{99}Ru resonance can be an important source of information, reflecting the degree of anisotropy of the electron distribution about the Ru nucleus. A highly unsymmetric electron distribution gives rise to a large electric field gradient (EFG) and, by virtue of an efficient quadrupolar relaxation mechanism, to a broadening of the signal. Linewidths up to several kHz are not uncommon[10] and, as with many other quadrupolar transition-metal nuclei,[1b] the resonances may even become too broad to be detected. Computed EFGs have been used before to rationalize observed trends in ^{91}Zr and ^{71}Ga linewidths.[11] A corresponding study is now included for selected ruthenium complexes.

Computational Details

Methods and basis sets correspond to those used in the previous studies of second-row transition-metal complexes:[6, 9] Geometries have been fully optimized in the given symmetry at the BP86/ECP1 level, that is, employing the exchange and correlation functionals of Becke[12] and Perdew,[13] respectively, together with a fine integration grid (75 radial shells with 302 angular points per shell), relativistic effective core potentials with the corresponding valence basis sets for Ru,[14] K,[15] Sn,[16] and I[16, 17] (contraction schemes [6s5p3d], [2s2p], [2s2p1d], and [2s2p1d], respectively), and a standard 6-31G* basis set[18] for all other elements. The geometry of **14** was optimized with an RI (resolution of identity)-DFT implementation in the TURBOMOLE program[19] that used a slightly different quadrature (grid 3)[20] and auxiliary basis sets optimized for the corresponding orbital basis sets[21] (polarization functions in the orbital basis sets of the phenyl groups have been omitted). Geometries are given as Supporting Information in the form of cartesian coordinates.

Magnetic shieldings σ have been evaluated for the BP86/ECP1 geometries with a recent implementation of the GIAO (gauge-including atomic orbitals)-DFT method,[22] that involves the functional combinations according to Becke[12] and Perdew and Wang[23] (denoted BPW91) or Becke (hybrid)[24] and Lee, Yang, and Parr,[25] (denoted B3LYP), together with basis II′, that is a [16s10p9d] all-electron basis for Ru, contracted from the well-tempered 22s14p12d set of Huzinaga and Klobukowski[26] and augmented with two d-shells of the well-tempered series, a [9s5p1d] basis on K, contracted from the 14s9p set of Wachters[27] and augmented with one set of d-functions (exponent 0.1), and the recommended IGLO-basis II[28, 29] on all other atoms except H, for which a double-zeta basis was used ([2s] contraction[28]); for **14**, the corresponding double-zeta basis was also employed for the phenyl carbon atoms (designated basis II″). The absolute shielding of the reference, aqueous $[K_4Ru(CN)_4]$, has been evaluated from the correlation of computed σ vs. experimental δ values (taken from refs. [10, 30]) for the set of compounds in this study (cf. the procedure for theoretical ^{103}Rh chemical shifts[6]), resulting in σ(standard) values of -488 and -1001 ppm at the GIAO-BPW91 and GIAO-B3LYP level, respectively.

We computed EFGs at the B3LYP/II′ level, employing the BP86/ECP1 geometries. The largest component of the EFG, q_{zz} (reported in atomic units; 1 au $= 9.717365 \times 10^{21}$ V m^{-2} for conversion into *eq* values), and the asymmetry parameter, $\eta = (q_{xx} - q_{yy})/q_{zz}$, are given. In addition, EFGs have been evaluated with a smaller basis set (denoted AE1) consisting of the same all-electron basis on Ru as in basis II′, but employing the pseudopotentials and basis sets from basis ECP1 on the ligands. In some instances, X-ray derived geometries have been used in the EFG computations. In these cases, hydrogen atoms have been added at standard positions (using CH bond distances of 1.10 Å). Polarization functions on phenyl or methyl groups in the Ru–XR_3 moieties (X = Sn, Pb;[31] R = Me, Ph) have been omitted. All computations, except for the RI-DFT optimization, employed the Gaussian series of programs.[32]

Results and Discussion

1. Geometries: Optimized geometries for the test set **1**–**14** comprising inorganic and organometallic species are displayed in Figure 1, together with key geometrical parameters. Distances observed in the solid state are included where available.[33, 34, 35, 36, 37, 38] As frequently observed for similar types of compounds, metal–carbon distances are well described, whereas the lengths of bonds with heavier elements tend to be overestimated at the DFT level employed.[39] Deviations up to 6 pm are not uncommon (e.g. the Ru–Ru distance in **7**). There is one spectacular error, however, namely the Ru–I bond length in **4a**, which is overestimated by as much as 10 pm (Figure 1).[40] In contrast, normal deviations relative to experiment are found for the optimized Ru–I distances in **10** and **12**, ca. 4–6 pm. A possible reason for the error in **4a** is the failure of the BP86 functional (or rather, the constituent exchange part)[41] to account for dispersion effects. The latter would counterbalance the closed-shell repulsion between the iodine atoms[42] and, in combination with a fairly flat stretching potential, serve to shorten the bonds. In fact, a considerably shorter Ru–I bond, 2.777 Å, is computed for **4a** at the MP2/ECP1 level (which includes large parts of the dispersion forces). For consistency, BP86 geometries have been employed in the NMR computations below. Evidently, special consideration must be given to the geometry dependence of the computed properties in **4**.

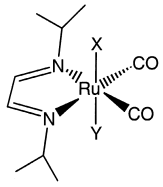

	X	Y
9	Cl	Me
10	I	Me
11	Cl	Cl
12	I	I
13	$SnMe_3$	$SnMe_3$
14	$SnPh_3$	$SnPh_3$
15	$SnPh_3$	Cl
16	$PbPh_3$	Cl

2. Chemical shifts: Absolute and relative ^{99}Ru chemical shifts, computed at the GIAO-BPW91 and -B3LYP levels are summarized in Table 1. The experimental standard, a 1M (or saturated) aqueous solution of $[K_4Ru(CN)_6]$, is difficult to model theoretically. Hence, the reference shielding value was evaluated from σ_{calcd} vs. δ_{exp} correlations as detailed in the computational section. Incidentally, the data computed for **2** as a model for the standard fit quite well into the correlations (see graphical representation in Figure 2), whereas a substantial deshielding is obtained for an isolated $[Ru(CN)_6]^{4-}$ tetraanion (ca. 450 and 600 ppm at the GIAO-BPW91 and -B3LYP levels, respectively).

The calculated δ values are plotted against the experimental data in Figure 2. The best accord with experiment is obtained at the GIAO-B3LYP level, as evidenced by the ideal slope of the δ_{calcd} vs. δ_{exp} linear regression, and by the relatively small mean absolute deviation, 120 ppm (Table 1, Figure 2a). The latter mean error corresponds to only 2% of the total chemical-shift range covered, ca. 5800 ppm, and can be considered quite satisfactory. Ruthenium thus joins the group of transition-metal nuclei mentioned in the introduction[6, 7, 8]

 © WILEY-VCH Verlag GmbH, D-69451 Weinheim, 2000 0947-6539/00/0617-3273 $ 17.50+.50/0

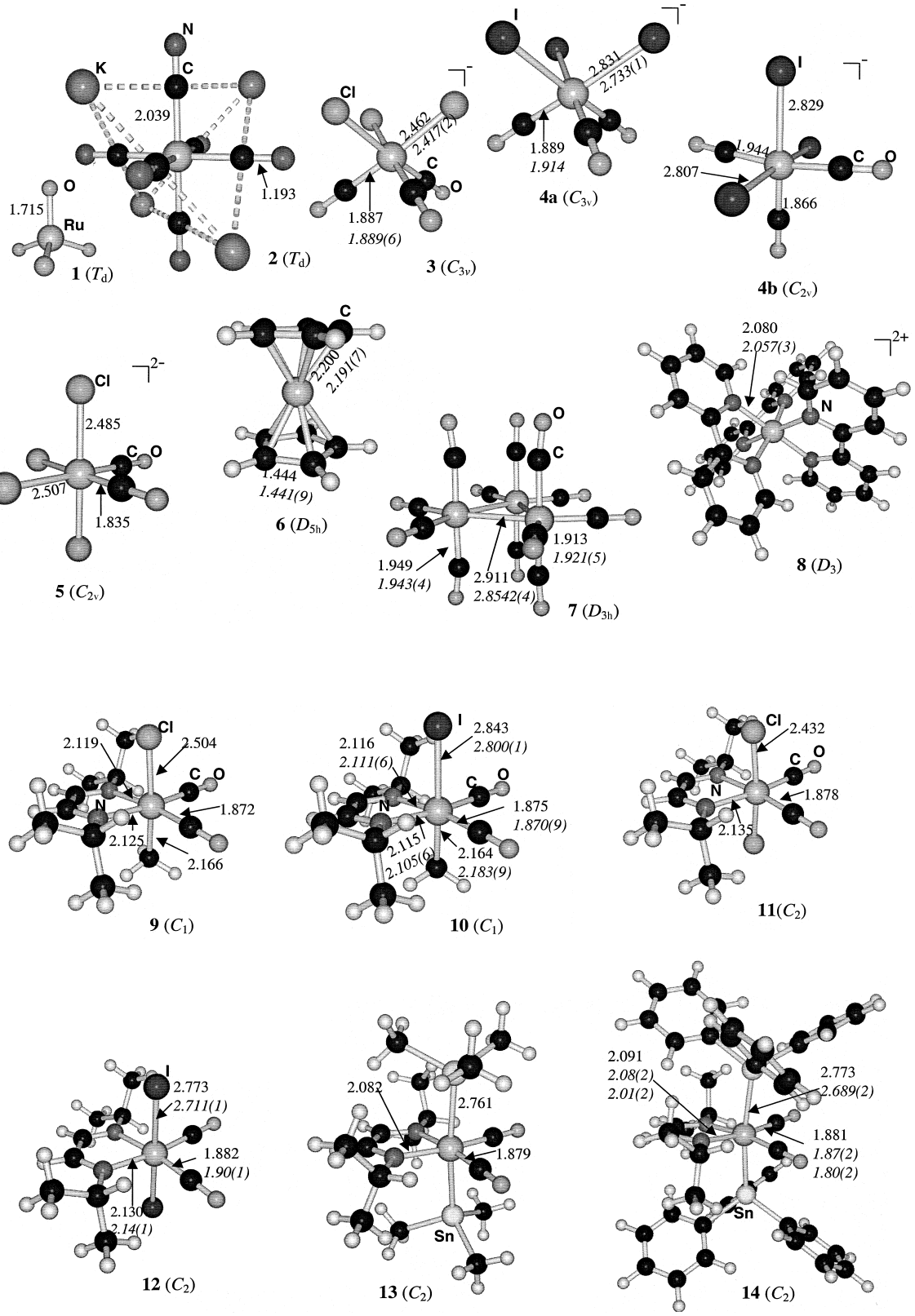

Figure 1. BP86/ECP1 optimized geometries of compounds **1**–**14** including key geometrical parameters (bond lengths in Å), together with the corresponding averaged data from experiment, where available (*in italics*).

for which the B3LYP hybrid functional outperforms "pure" density functionals in chemical-shift calculations. The opposite has been found for ^{95}Mo,[9] the only exception encountered so far.

The very good performance of the GIAO-DFT method is particularly noteworthy because in four compounds of the test set, heavier elements (I and Sn) are bonded to Ru. In such a case relativistic effects, which are not accounted for in the

© WILEY-VCH Verlag GmbH, D-69451 Weinheim, 2000
0947-6539/00/0617-3274 $ 17.50+.50/0 *Chem. Eur. J.* **2000**, *6*, No. 17

Table 1. Theoretical absolute (σ) and relative (δ) ^{99}Ru chemical shifts[a] in complexes **1**–**14**, together with experimental data.[b]

Molecule	σ		δ		
	BPW91	B3LYP	BPW91	B3LYP	Expt.[b]
RuO_4 (**1**)	−2525	−3097	2021	2096	1976
$K_4[Ru(CN)_6]$ (**2**)	−459	−1048	−44	47	0
fac-$[Ru(CO)_3Cl_3]^-$ (**3**)	−979	−1548	476	547	816[c]
fac-$[Ru(CO)_3I_3]^-$ (**4a**)	−553	−1077	49	77	56[c]
mer-$[Ru(CO)_3I_3]^-$ (**4b**)	−657	−1368	153	368	356[c]
cis-$[Ru(CO)_2Cl_4]^{2-}$ (**5**)	−2202	−3162	1698	2162	2537[d]
$[Ru(C_5H_5)_2]$ (**6**)	654	169	−1157	−1169	−1270
$[Ru_3(CO)_{12}]$ (**7**)	477	226	−981	−1227	−1208
$[Ru(bipy)_3]^{2+}$ (**8**)	−4443	−5760	3939	4759	4518[e]
$[Ru(CO)_2(i\text{Pr-DAB})(Cl)(CH_3)]$ (**9**)	−1321	−1864	817	863	794
$[Ru(CO)_2(i\text{Pr-DAB})(I)(CH_3)]$ (**10**)	−1073	−1591	569	593	771
$[Ru(CO)_2(i\text{Pr-DAB})(Cl)_2]$ (**11**)	−1986	−2858	1483	1857	1993
$[Ru(CO)_2(i\text{Pr-DAB})(I)_2]$ (**12**)	−1333	−2104	829	1103	1036
$[Ru(CO)_2(i\text{Pr-DAB})(SnMe_3)_2]$ (**13**)	−446	−772	−58	−229	−316
$[Ru(CO)_2(i\text{Pr-DAB})(SnPh_3)_2]$ (**14**)	−642	−997	138	−2	−116
Slope[f]	0.83	0.99			
Intercept[f]	−504	−1000			
Mean absolute deviation			275	133	

[a] Employing GIAOs, basis II (**14**: basis II″), and BP86/ECP1 geometries (bipy = 2,2-bis(pyridine); DAB = 1,3-diazabutadiene). [b] From refs. [10, 30]; the ^{99}Ru NMR spectra of **9**–**14** were recorded in THF solutions at 313 K. That for compound **8** was measured in D_2O at 313 K and that for **6** was recorded in chloroform solution at 313 K. [c] Counterion: bis(triphenylphosphine)iminium cation in acetone. [d] Counterion: Cs^+ in D_2O. [e] Counterion: Cl^- in D_2O. [f] From the σ_{calcd} vs. δ_{exp} linear regression.

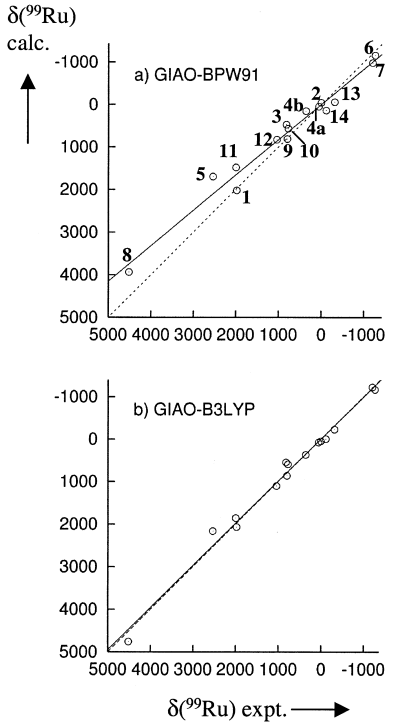

Figure 2. Plot of computed (basis II′ for BP86/ECP1 optimized geometries) vs. experimental ^{99}Ru chemical shifts: a) GIAO-BPW91 level; b) GIAO-B3LYP level. Linear regression lines (solid) and ideal lines with the slope 1 (dashes) are included.

present approach, can become important and can actually dominate the observed trends. The halomethanes CX_4 are the archetypical example; the unusually high carbon shielding in CI_4 is almost exclusively due to relativity-induced spin–orbit (SO) coupling.[43] The mechanism of such heavy-atom effects on chemical shifts of neighboring nuclei is now well understood and, because of the dominating Fermi contact term, nicely lends itself to a simple analogy with spin–spin coupling constants.[44] As the latter increase with the s-orbital contributions in the bonds between the nuclei, so does the importance of SO effects on the nuclear shielding. Bonds involving early transition metals in high oxidation states have only small metal s-orbital contributions and, consequently, SO effects on the metal shifts are negligible, as for example in TiI_4.[45] The bonding of middle or late transition metals such as Ru is different, however. Noticeable s(Ru) character is indeed present in the Ru–Sn bonds in **13** and related compounds, as evidenced by detectable $^1J(^{117/119}Sn,^{99}Ru)$ coupling constants on the order of 250–340 Hz.[10] In the absence of lone pairs and high-lying bonding MOs on the heavy atom, SO effects on neighboring magnetic shieldings are indicated to be small[46] and can, thus, probably be neglected for the tin derivatives. For iodo species, the situation is less clear beforehand. Inspection of the natural localized MOs (NLMOs) from a natural bond orbital (NBO) analysis[47] reveals some s character on Ru in the Ru–I bonds, up to 22% of the Ru AOs in **4a** (B3LYP/AE1 level). However, the bonds are strongly polarized towards I,[48] leaving much less net s character on the metal.[49] Thus, the nonrelativistic evaluation of the ^{99}Ru properties should still be possible (in particular as far as general trends are concerned), but this neglect of relativity should always be kept in mind as a potential source of error.[50]

In view of this discussion, and recalling the spectacular deviation for the Ru–I bond length in **4a**, the good performance of the iodo compounds in Table 1 might actually be due to a fortuitous cancellation of these errors. From chemical-shift calculations for appropriately distorted structures, a bond-length shielding derivative of ca. 3600 ppm Å^{-1} is obtained for the Ru–I bond in **4a**.[51] The excessively enlarged optimized Ru–I distance should thus translate into spurious deshielding of several hundred ppm which is, however, not

apparent in the data of Table 1 and Figure 1. Despite these uncertainties it is noteworthy that the difference in $\delta(^{99}Ru)$ between the isomers **4a** and **4b** is well reproduced by the present theoretical approach, suggesting transferability of potential errors. With this caveat in mind it appears that trends in ^{99}Ru chemical shifts can be well described at the GIAO-B3LYP level.

3. Electric field gradients: Excessive line broadening due to efficient quadrupolar relaxation is one of the main obstacles in transition-metal NMR spectroscopy. When relaxation is dominated by this mechanism, the linewidth $\Delta\nu_{1/2}$ should be dependent on the largest EFG component q_{zz}, on the asymmetry parameter η, defined as $(q_{xx}-q_{yy})/q_{zz}$, and on the molecular correlation time τ_c (which measures the orientational mobility of a molecule and usually increases with molecular size), as described in Equation (1).[52] For

$$\Delta\nu_{1/2} \propto q_{zz}^2\left(1+\frac{\eta^2}{3}\right)\tau_c \qquad (1)$$

several classes of Ru compounds, some of us observed characteristic variations in the ^{99}Ru NMR linewidths[10] that we attributed to changes in τ_c and in the EFGs. The former could be determined experimentally for some compounds, but the latter was found "difficult to quantify".[10] In fact, it was the need for a reliable estimate of this property which stimulated the present study.

Even though the EFG, in contrast to the chemical shift, is a simple expectation value and a typical ground-state property, accurate calculations require the use of large basis sets and inclusion of electron correlation at fairly sophisticated levels.[53] In addition, relativistic effects may become important for heavier elements.[54] On the other hand, trends within a given set of compounds can often be well reproduced qualitatively at lower or intermediate levels, such as Hartree–Fock[11] or DFT.[53c, 55] For consistency with the chemical-shift calculations discussed above, we have computed EFGs employing the B3LYP combination of density functionals, obtaining the results summarized in Table 2.

As has been observed previously,[10] certain trends in linewidths of the octahedral *i*Pr-DAB (DAB = 1,3-diazabutadiene) complexes are quite unexpected: for instance, why do the monohalogeno methyl complexes **9** and **10** have such sharp lines? Why is the resonance of the bis(iodo) compound **12** so much broader than those of the larger tin derivatives? And why, among the latter, does the bulkier phenyl derivative **14** have a narrower line than the corresponding methyl species **13**? None of these observations can be reconciled with the correlation time as being the dominant factor in Equation (1), according to which larger molecules should display broader lines. Consequently, it must be the EFG that causes these variations.

As a first test of this assumption, we carried out EFG computations for compounds **10**, **12**, **14**–**16** employing the medium-sized AE1 basis and geometries derived from X-ray crystallography,[38, 56] as well as for the solid-state structure of **4a**[34] for comparison (fourth entry in Table 2). The agreement between computed q_{zz} and experimental $\Delta\nu_{1/2}$ values is only moderate: while the smallest EFGs are indeed obtained for **4a** and **10**, the species with the narrowest lines in this set, the largest q_{zz} is computed not for **12**, but rather for **14**, which has a much sharper line. No experimental structure is known for the trimethyltin derivative **13**; as a first estimate (before the actual BP86/ECP1 optimization), this has been constructed from the solid-state structure of **14** by replacing the phenyl groups with methyl groups and adjusting the Ru–Sn and Sn–C bond lengths to values typical for other Ru–$SnMe_3$ species (2.66 and 2.15 Å, respectively), leaving all other parameters unchanged. The estimated q_{zz} value obtained this way for **13**, however, is smaller than that for **14**, that is in reverse order to the observed linewidths (Table 2). Thus, the large variations in $\Delta\nu_{1/2}$ for **12**–**14** are not reflected in the computed EFGs when experimental or estimated geometries are employed.

Table 2. Computed (B3LYP level) EFG parameters[a] of the Ru atoms in complexes **1**–**16** together with experimental ^{99}Ru NMR linewidths where available.[b]

Molecule	q_{zz}			(η)	$\Delta\nu_{1/2}$
	AE1//X-ray[c]	AE1	II′	II′	Exp.[b]
$[RuO_4]$ (**1**)		0	0	(0)	1
$K_4[Ru(CN)_6]$ (**2**)		0	0	(0)	2
fac-$[Ru(CO)_3Cl_3]^-$ (**3**)		0.248	0.255	(0)	112
fac-$[Ru(CO)_3I_3]^-$ (**4a**)	0.100	0.003	0.010	(0)	10
mer-$[Ru(CO)_3I_3]^-$ (**4b**)		1.278	1.209	(0.861)	75
cis-$[Ru(CO)_2Cl_4]^{2-}$ (**5**)		1.070	0.966	(0.355)	
$[Ru(C_5H_5)_2]$ (**6**)			1.858	(0)	850[d]
$[Ru_3(CO)_{12}]$ (**7**)			0.129	(0.659)	75
$[Ru(bipy)_3]^{2+}$ (**8**)			0.300	(0)	140
$[Ru(CO)_2$(*i*Pr-DAB)$(Cl)(Me)]$ (**9**)		0.374	0.393	(0.887)	40
$[Ru(CO)_2$(*i*Pr-DAB)$(I)(Me)]$ (**10**)	0.223	0.243	0.256	(0.559)	30
$[Ru(CO)_2$(*i*Pr-DAB)$(Cl)_2]$ (**11**)		0.746	0.654	(0.623)	695
$[Ru(CO)_2$(*i*Pr-DAB)$(I)_2]$ (**12**)	0.600	1.001	0.940	(0.397)	1435
$[Ru(CO)_2$(*i*Pr-DAB)$(SnMe_3)_2]$ (**13**)	(0.581)[e]	0.382	0.385	(0.331)	100
$[Ru(CO)_2$(*i*Pr-DAB)$(SnPh_3)_2]$ (**14**)	0.644	0.256	0.273[f]	(0.609)[f]	96
$[Ru(CO)_2$(*i*Pr-DAB)$(SnPh_3)(Cl)]$ (**15**)	0.361				660
$[Ru(CO)_2$(*i*Pr-DAB)$(PbPh_3)(Cl)]$ (**16**)	0.304				800

[a] Largest component of the EFG, q_{zz}, in au, and asymmetry parameter η; the calculations employed basis sets as indicated and, except where otherwise noted, BP86/ECP1 geometries. [b] From refs. [10, 30a]. [c] Employing X-ray derived geometries. [d] 30 °C, 790 Hz at 40 °C (redetermined in this work, ref. [58]). [e] Estimated (see text). [f] Basis II″.

© WILEY-VCH Verlag GmbH, D-69451 Weinheim, 2000
0947-6539/00/0617-3276 $ 17.50+.50/0 *Chem. Eur. J.* **2000**, *6*, No. 17

Since light atoms in the vicinity of heavier ones are more difficult to locate by X-ray diffraction techniques, the experimental structures are associated with notable uncertainties. For instance, the two (formally equivalent) Ru–C(O) bond lengths in **14** are refined to 1.80(2) and 1.87(2) Å,[38] that is, they are identical within experimental error (taken as 3σ), yet they differ by 7 pm. The same holds true for the two Ru–N distances, 2.08(2) and 2.01(2) Å. It is possible that such (presumably artificial) asymmetries in the molecular structure result in a spurious increase of the computed EFG at the central metal position. When the fully optimized DFT geometries of **13** and **14** are employed instead (C_2 symmetry imposed), the q_{zz} values are indeed significantly reduced (compare the entries in the second and third columns of Table 2). In contrast, for the iodo species **10** and **12** the use of optimized geometries results in somewhat larger computed EFGs. In the series **9**–**14**, the trend in the EFG values computed at the B3LYP/AE1 level parallels that in the $\Delta\nu_{1/2}$ data, confirming the dominance of the former in determining the line shape. In particular, the rather narrow line observed for the bulky bis(triphenyltin) complex can be traced back to a fairly small EFG.

Interestingly, the optimized geometries of **13** and **14** differ in the relative orientation of the SnR_3 groups: viewed along the Sn···Sn line, the substituents at tin appear nearly staggered in **14** (as found in the solid), but are almost eclipsed in **13** (see Figure 3). Apparently, the methyl substituents at tin

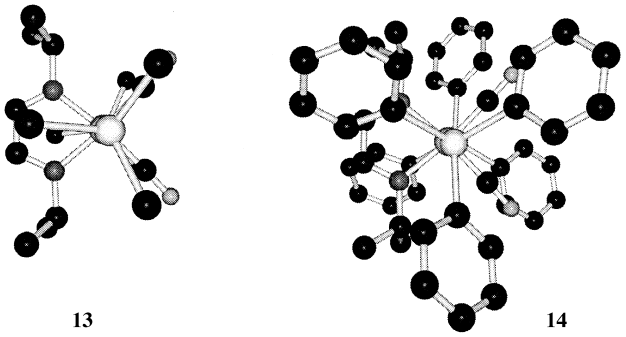

Figure 3. Conformations of the SnR_3 moieties in **13** and **14** (BP86/ECP1 optimized), viewed along the Sn···Sn line (hydrogen atoms have been omitted for clarity).

can fit almost symmetrically into the void between the *i*Pr groups, whereas the phenyl moieties cause larger distortions.

For a number of the *i*Pr-DAB complexes, correlation times τ_c have been determined from T_1 measurements, affording values of 43, 8.4, and 18 ($\times 10^{-12}$ s each) for **14**, **9**, and **12**, respectively.[10] When the corresponding observed linewidths are divided by these numbers according to Equation (1), the ratio of the pure EFG contributions should be 1:2.2:35 in the same sequence of compounds. The corresponding relative ratio of the squared q_{zz} values from Table 1 (II′ level) is 1:2.1:12, in good qualitative (albeit not fully quantitative) accord with the EFG contribution ratio.

Subsequently, EFGs have been evaluated at the B3LYP/AE1 level for some, and at the B3LYP/II′ level for all optimized geometries of **1**–**14**. An increase of the basis set on the ligands about Ru has usually only a small effect on the q_{zz} values (compare third and fourth columns in Table 2). In addition, the asymmetry parameters η obtained with basis II′ are included in Table 2 (values in parentheses). This parameter enters Equation (1) in the factor $(1+\frac{\eta^2}{3})$, which can only assume values between 1 and 1⅓ and is therefore not expected to govern the general trends observed. A plot of the principal EFG contribution, the factor q_{zz}^2 (B3LYP/II′ level), versus the observed linewidths is presented in Figure 4. One should bear in mind that no perfect correlation can be expected because the experimental $\Delta\nu_{1/2}$ data contain the dependence on τ_c and, thus, on molecular size, viscosity of the solvent, concentration, and temperature. Of these parameters at least the first two usually vary from one experiment to the other.

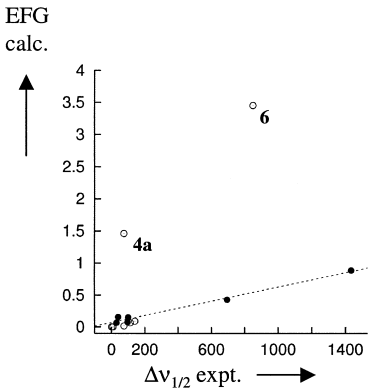

Figure 4. Plot of the computed EFG contributions to $\Delta\nu_{1/2}$ (B3LYP/II′ level for BP86/ECP1 optimized geometries) vs. the actual observed linewidths. Filled circles: *i*Pr-DAB complexes **9**–**14**. The linear regression line for the latter is shown.

Most data points in Figure 4 are clustered in the lower left, that is, narrow lines are indeed associated with small EFGs. The above-mentioned common trends in $\Delta\nu_{1/2}$ and q_{zz} for the *i*Pr-DAB complexes **9**–**14** are reflected in the fairly good correlation of the corresponding points in Figure 4 (filled circles). However, no general correlation is found for all compounds in the set, and for the two labeled data points much larger EFGs are computed than expected from the observed linewidths.

The first of these is the *mer*-isomer of $[Ru(CO)_3I_3]^-$ (**4b**). Essentially the same q_{zz} values are obtained with basis AE1 and II′, that is, whether or not scalar relativistic effects due to iodine are included (Table 2). It has been noted above that the optimized Ru–I bond length of the *fac* isomer **4a** is considerably in error. When the Ru–I bonds in **4b** are adjusted accordingly (i.e., reduced by 10 pm), one arrives at a somewhat smaller EFG ($q_{zz} = 0.902$ au, B3LYP/II′ level) than for the fully optimized structure. In the set of *i*Pr-DAB compounds, such a value would correspond to a linewidth well above 1 kHz, two orders of magnitude larger than what is observed. The reason for this offset remains unknown.

The second problem case is ruthenocene (**6**): it has the largest computed EFG of all species studied so far, $q_{zz} =$ 1.86 au (Table 2),[57] but no excessively broadened line. [58] For this compound (to our knowledge the only one among **1**–**16**) an independent check of the computed EFG is possible

because the Mössbauer quadrupole splitting ΔE_Q has been measured.[59] For $\eta = 0$, and assuming, as commonly accepted,[60] that the splitting can be described as doublet owing to the $I = 3/2$ excited state of ^{99}Ru, this quantity is given by Equation (2), where $Q_{3/2}$ is the nuclear quadrupole moment.

$$\Delta E_Q = \tfrac{1}{2} e^2 q_{zz} Q_{3/2} \quad (2)$$

With the reference data available,[61] $q_{zz} = 1.15$ au can be deduced from the measured ΔE_Q for **1**. While the B3LYP value is larger by a sizeable amount (60%) it appears nevertheless to be of the correct order of magnitude.[62] The EFGs of **6** and of three additional molecules[63] have been computed at the same level and are compared with the Mössbauer results in Table 3.

Even though three of the four molecules in Table 3 are charged species, in which effects of the crystal lattice on the EFG can probably not be fully neglected, it is obvious that the general trend is well reproduced at the B3LYP/II′ level. Thus, ruthenocene (**6**) should indeed have the largest EFG among

Table 3. Comparison of experimental and computed EFG parameters.

Molecule	ΔE_Q(exp.)[a] [mm s^{-1}]	q_{zz}(exp.)[b] [au]	q_{zz}(B3LYP) [au]
$[Ru(bipy)_3]^{2+}$ (**8**)	(< 0.08)[c]	(< 0.21)	0.300
$[RuO_4]^-$ (**17**)	0.37(2)[d]	0.99(5)	1.613
$[Ru(C_5H_5)_2]$ (**6**)	0.43(2)	1.15(5)	1.858
$[RuCl_4N]^-$ (**18**)	1.60(6)[e]	4.27(16)	4.386

[a] Mössbauer quadrupole splittings from ref. [59]. [b] See footnote [61] for conversion from ΔE_Q values. [c] Counterion $[ClO_4]^-$; no quadrupole splitting could be detected, so therefore it must be below 0.08(8) mm s^{-1}, the smallest value reported (at a natural linewidth of 0.15 mm s^{-1}). [d] Counterion K^+. [e] Counterion $[NBu_4]^+$.

the test set **1**–**14**, and the narrow line compared to, say, **12** must at least in part be due to a reduced correlation time. However, the EFG and line width data in Figure 4 can only be reconciled with each other by the assumption of a very low τ_c value for **6**.

Conclusion

We have presented an assessment of gradient-corrected and hybrid DFT levels for the computation of ^{99}Ru NMR properties of a representative set of inorganic and organometallic Ru compounds. For the description of chemical shifts, the B3LYP hybrid functional is superior to the pure BPW91 functional; this also applies to all other transition metals studied so far, with the sole exception of ^{95}Mo. The nonrelativistic treatment of heavier elements bonded to Ru does not appear to be particularly problematic, but the errors possibly introduced this way should eventually be quantified.

Trends in EFGs assessed by Mössbauer quadrupole splittings can be reproduced qualitatively at the B3LYP/II′ level. The a priori prediction of NMR linewidths based on computed EFGs, however, appears difficult and is probably restricted to series of closely related compounds. For [Ru(CO)$_2$(*i*Pr-DAB)(X)(Y)] species, for instance, trends in computed EFGs at the central metal atom parallel those in the observed ^{99}Ru NMR linewidths, consistent with the dominant quadrupolar relaxation mechanism expected for this nucleus. However, subtle trends are only captured when optimized geometries, rather than estimated ones or solid-state structures, are employed.

In summary, we have identified the DFT levels necessary for the theoretical treatment of ^{99}Ru chemical shifts and, at least qualitatively and with less predictive power, linewidths. Such computations can be a valuable complement to ^{99}Ru NMR spectroscopy, which presents itself as a useful and versatile analytical tool for ruthenium compounds.

Acknowledgements

MB wishes to thank Prof. Dr. W. Thiel for his continuous support, Prof. Dr. M. Kaupp and Prof. Dr. V. G. Malkin for valuable suggestions, Dr. K. Angermund and F. Weigend for assistance with the Cambridge Structure Database and with TURBOMOLE, respectively, and the Deutsche Forschungsgemeinschaft for a Heisenberg fellowship. CJE and SG thank J. M. Ernsting for skilful technical assistance with NMR experiments, and the John van Geuns Foundation and the Council for Chemical Sciences of the Netherlands Organization for Scientific Research (CW-NWO) for financially supporting the acquisition of NMR spectrometers and probes. Calculations have been carried out on Silicon Graphics PowerChallenge, IBM RS 6000, and Compaq XP 1000 workstations (at the Organisch-chemisches Institut, Universität Zürich, ETH Zürich, and Max-Planck-Institut, Mülheim), as well as on a NEC-SX4 (CSCS, Manno, Switzerland).

[1] a) R. Benn, A. Rufinska, *Angew. Chem.* **1986**, *98*, 851–871; *Angew. Chem. Int. Ed. Engl.* **1986**, *25*, 861–881; b) *Transition Metal Nuclear Magnetic Resonance* (Ed.: P. S. Pregosin), Elsevier, Amsterdam, **1991**.
[2] W. von Philpsborn, *Chem. Soc. Rev.* **1999**, *28*, 95–105.
[3] See, for instance: *The Encyclopedia of Computational Chemistry* (Eds.: P. v. R. Schleyer, N. L. Allinger, T. Clark, J. Gasteiger, P. A. Kollman, H. F. Schaefer III, P. R. Schreiner), Wiley, Chichester, **1998**.
[4] T. Ziegler, *Can. J. Chem.* **1995**, *73*, 743–761.
[5] For recent reviews see: a) M. Kaupp, V. G. Malkin, O. L. Malkina, in *The Encyclopedia of Computational Chemistry* (Eds.: P. v. R. Schleyer, N. L. Allinger, T. Clark, J. Gasteiger, P. A. Kollman, H. F. Schaefer, III, P. R. Schreiner), Wiley, Chichester, **1998**, pp. 1857–1866; b) M. Bühl, M. Kaupp, V. G. Malkin, O. L. Malkina, *J. Comput. Chem.* **1999**, *20*, 91–105; c) G. Schreckenbach, T. Ziegler, *Theor. Chem. Acc.* **1998**, *99*, 71–82.
[6] M. Bühl, *Chem. Phys. Lett.* **1997**, *267*, 251–257.
[7] N. Godbout, E. Oldfield, *J. Am. Chem. Soc.* **1997**, *119*, 8065–8069.
[8] M. Bühl, F. A. Hamprecht, *J. Comput. Chem.* **1998**, *119*, 113–122.
[9] M. Bühl, *Chem. Eur. J.* **1999**, *5*, 3514–3522.
[10] S. Gaemers, J. van Slageren, C. M. O'Connor, J. G. Vos, R. Hage, C. J. Elsevier, *Organometallics* **1999**, *18*, 5238–5244.
[11] a) M. Bühl, G. Hopp, W. von Philipsborn, S. Beck, M. Prosenc, U. Rief, H.-H. Brintzinger, *Organometallics* **1996**, *15*, 778–785; b) M. Bühl, *Magn. Reson. Chem.* **1996**, *34*, 782–790.
[12] A. D. Becke, *Phys. Rev. A* **1988**, *38*, 3098–3100.
[13] a) J. P. Perdew, *Phys. Rev. B* **1986**, *33*, 8822–8824; b) J. P. Perdew, *Phys. Rev. B* **1986**,*34*, 7406.
[14] D. Andrae, U. Häussermann, M. Dolg, H. Stoll, H. Preuss, *Theor. Chim. Acta* **1990**, *77*, 123–141.
[15] P. Fuentealba, H. Preuss, H. Stoll, L. von Szentpaly, *Chem. Phys. Lett.* **1982**, *89*, 418–422.
[16] A. Bergner, M. Dolg, W. Küchle, H. Stoll, H. Preuss, *Mol. Phys.* **1993**, *80*, 1431–1441.
[17] Valence basis for I taken from: M. Kaupp, P. v. R. Schleyer, H. Stoll, H. Preuss, *J. Am. Chem. Soc.* **1991**, *113*, 6012–6020.

 © WILEY-VCH Verlag GmbH, D-69451 Weinheim, 2000 0947-6539/00/0617-3278 $ 17.50+.50/0

[18] a) W. J. Hehre, R. Ditchfield, J. A. Pople, *J. Chem. Phys.* **1972**, *56*, 2257–2261; b) P. C. Hariharan, J. A. Pople, *Theor. Chim. Acta.* **1973**, *28*, 213–222.

[19] R. Ahlrichs, M. Bär, M. Häser, H. Korn, M. Kölmel, *Chem. Phys. Lett*. **1989**, *154*, 165–169.

[20] O. Treutler, R. Ahlrichs, *J. Chem. Phys.* **1995**, *102*, 346–354.

[21] a) K. Eichkorn, O. Treutler, H. Öhm, M. Häser, R. Ahlrichs, *Chem. Phys. Lett*. **1995**, *240*, 283; b) K. Eichkorn, F. Weigend, O. Treutler, R. Ahlrichs, *Theor. Chem. Acc.* **1997**, *97*, 119–124; auxiliary bases have been obtained from Karlsruhe by ftp, see: http://www.chemie.uni-karlsruhe.de/PC/Theochem (SVP-optimized in conjunction with 6-31G* basis).

[22] J. R. Cheeseman, G. W. Trucks, T. A. Keith, M. J. Frisch, *J. Chem. Phys.* **1996**, *104*, 5497–5509.

[23] a) J. P. Perdew, in *Electronic Structure of Solids* (Eds.: P. Ziesche, H. Eischrig), Akademie, Berlin, **1991**; b) J. P. Perdew, Y. Wang, *Phys. Rev. B* **1992**, *45*, 13244–13249.

[24] A. D. Becke, *J. Chem. Phys.* **1993**, *98*, 5648–5642.

[25] C. Lee, W. Yang, R. G. Parr, *Phys. Rev. B* **1988**, *37*, 785–789.

[26] S. Huzinaga, M. Klobukowski, *J. Mol. Struct.* **1988**, *167*, 1–210.

[27] A. J. H. Wachters, *J. Chem. Phys.* **1970**, *52*, 1033–1036.

[28] W. Kutzelnigg, U. Fleischer, M. Schindler, in *NMR Basic Principles and Progress, Vol. 23*, Springer, Berlin, **1990**, pp. 165–262.

[29] Sn and I basis sets are constructed from Huzinaga basis functions, contracted and augmented (no f functions have been included in the present work) to [12s11p9d]: a) U. Fleischer, unpublished; these basis sets are constructed analogously to those described in: b) U. Fleischer, Ph.D. thesis, University of Bochum (Germany), 1992; c) M. Bühl, W. Thiel, U. Fleischer, W. Kutzelnigg, *J. Phys. Chem*. **1995**, *99*, 4000–4007.

[30] a) R. W. Dykstra, A. M. Harrison, *J. Magn. Reson*. **1982**, *46*, 338–342; b) C. Brevard, P. Granger, *Inorg. Chem*. **1982**, *22*, 532–535.

[31] Pb is described with a MEFIT ECP together with a 2s2s1d valence basis: W. Küchle, M. Dolg, H. Stoll, H. Preuss, *Mol. Phys.* **1991**, *74*, 1245–1263.

[32] a) M. J. Frisch, G. W. Trucks, H. B. Schlegel, P. M. W. Gill, B. G. Johnson, M. A. Robb, J. R. Cheeseman, T. Keith, G. A. Petersson, J. A. Montgomery, K. Raghavachari, M. A. Al-Laham, V. G. Zakrzewski, J. V. Ortiz, J. B. Foresman, C. Y. Peng, P. Y. Ayala, W. Chen, M. W. Wong, J. L. Andres, E. S. Replogle, R. Gomperts, R. L. Martin, D. J. Fox, J. S. Binkley, D. J. DeFrees, J. Baker, J. J. P. Stewart, M. Head-Gordon, C. Gonzales, J. A. Pople, Gaussian 94, Gaussian, Pittsburgh (PA), **1995**; b) M. J. Frisch, G. W. Trucks, H. B. Schlegel, G. E. Scuseria, M. A. Robb, J. R. Cheeseman, V. G. Zakrzewski, J. A. Montgomery, R. E. Stratman, J. C. Burant, S. Dapprich, J. M. Millam, A. D. Daniels, K. N. Kudin, M. C. Strain, O. Farkas, J. Tomasi, V. Barone, M. Cossi, R. Cammi, B. Mennucci, C. Pomelli, C. Adamo, S. Clifford, J. Ochterski, G. A. Petersson, P. Y. Ayala, Q. Cui, K. Morokuma, D. K. Malick, A. D. Rabuck, K. Raghavachari, J. B. Foresman, J. Cioslowski, J. V. Ortiz, A. G. Baboul, B. B. Stefanov, C. Liu, A. Liashenko, P. Piskorz, I. Komaromi, R. Gomperts, R. L. Martin, D. J. Fox, T Keith, M. A. Al-Laham, C. Y. Peng, A. Nanayakkara, C. Gonzalez, M. Challacombe, P. M. W. Gill, B. G. Johnson, W. Chen, M. W. Wong, J. L. Andres, C. Gonzales, M. Head-Gordon, E. S. Replogle, J. A. Pople, Gaussian 98, Gaussian, Pittsburgh (PA), **1998**.

[33] Compound **3**: Averaged values taken from a) P. Teulon, J. Roziere, *Z. Anorg. Allg. Chem*. **1981**, *483*, 219–224 (counterions $H_3O^+/H_2O/SbCl_3$); b) C. S. Griffith, G. A. Koutsantonis, C. L. Raston, J. P. Selegue, B. W. Skelton, A. H. White, *J. Organomet. Chem*. **1996**, *518*, 197–202 (counterion $[RuCp(CO)_3]^+$).

[34] Compound **4a**: A. M. R. Galletti, G. Braca, S. Brana, F. Marchetti, *J. Mol. Catal*. **1985**, *32*, 291–308 (counterion (18-crown-6)K^+).

[35] Compound **6**: P. Seiler, J. D. Dunitz, *Acta Crystallogr. B* **1980**, *36*, 2946–2950.

[36] Compound **7**: M. R. Churchill, F. J. Hollander, J. P. Hutchinson, *Inorg. Chem*. **1977**, *16*, 2655–2659.

[37] Compound **8**: Averaged values taken from a) D. P. Rillema, D. S. Jones, H. A. Levy, *J. Chem. Soc. Chem. Commun.* **1979**, 849–851 (counterion PF_6^-); b) J. M. Harrowfield, A. N. Sobolev, *Aust. J. Chem*. **1994**, *47*, 763–767 (counterion ClO_4^-); c) E. Krausz, H. Riesen, A. D. Rae, *Aust. J. Chem*. **1995**, *48*, 929–954 (counterion ClO_4^-).

[38] a) Compound **10**: C. J. Kleverlaan, D. J. Stufkens, J. Fraanje, K. Goubitz, *Eur. J. Inorg. Chem*. **1998**, 1243–1251; b) Compound **12**: H. A. Nieuwenhuis, M. C. E. van de Ven, D. J. Stufkens, A. Oskam, K. Goubitz, *Organometallics* **1995**, *14*, 780–788; c) Compound **14**: M. P. Aarnts, M. P. Wilms, K. Peelen, J. Fraanje, K. Goubitz, F. Hartl, D. J. Stufkens, E. J. Baerends, A. Vlcek, *Inorg. Chem*. **1996**, *35*, 5468–5477.

[39] See for instance: M. R. Bray, R. J. Deeth, V. J. Paget, P. D. Sheen, *Int. J. Quantum Chem.* **1996**, *61*, 85–91.

[40] Inclusion of diffuse functions on I (which could improve the description of this anionic system) has almost no effect on the optimized bond lengths. Scalar relativistic effects are included through the pseudopotentials on the heavier elements, which is usually sufficient (see for instance: G. Frenking, I. Antes, M. Böhme, S. Dapprich, A. W. Ehlers, V. Jonas, A. Neuhaus, M. Otto, R. Stegmann, A. Veldkamp, S. F. Vyboishchikov, in *Reviews in Computational Chemistry, Vol. 8* (Eds: K. B. Lipkowitz, D. B. Boyd), VCH, New York, **1996**, pp. 63–144).

[41] See for instance: Y. Zhang, W. Pan, W. Yang, *J. Chem. Phys.* **1997**, *107*, 7921–7925.

[42] Such effects are apparent e.g. in the thermochemistry of perchloroalkanes: J. Cioslowski, G. Liu, D. Moncrieff, *J. Phys. Chem. A* **1998**, *102*, 9965–9969.

[43] See for instance: a) V. G. Malkin, O. L. Malkina, D. R. Salahub, *Chem. Phys. Lett.* **1996**, *261*, 335–345; the same is found, for example, for the silicon shielding in SiI_4: b) H. Nakatsuji, T. Nakajima, M. Hada, H. Takashima, S. Tanaka, *Chem. Phys. Lett*. **1995**, *247*, 418–424.

[44] M. Kaupp, O. L. Malkina, V. G. Malkin, P. Pyykkö, *Chem. Eur. J*. **1998**, *4*, 118–126.

[45] H. Nakatsuji, Z.-M. Hu, T. Nakajima, *Chem. Phys. Lett*. **1997**, *275*, 429–436.

[46] M. Kaupp, O. L. Malkina, V. G. Malkin, *J. Comput. Chem*. **1999**, *20*, 1304–1313.

[47] Review: A. E. Reed, L. A. Curtiss, F. Weinhold, *Chem. Rev.* **1988**, *88*, 899–926.

[48] In fact, an unconstrained NLMO search finds no bonds between Ru and I in **4a**; rather, an ionic description results, with lone pairs on I containing small contributions (ca. 15%) from the metal. The s(Ru) contributions mentioned in the text are obtained when a Ru–I bonding MO is enforced using the CHOOSE keyword in Gaussian 94; in this option, enforced NLMO populations of ca. 40% and 60% are assigned to Ru and I, respectively.

[49] At the same level, the s(C) contribution in the C–I NLMO of CI_4 is 31%, with a polarization of the MO towards C (total populations ca. 60% and 40% on C and I, respectively).

[50] The relativistic effects of second-row transition-metal nuclei on their own shielding constants are noticeable, but cancel to a large extent when relative chemical shifts, i.e. shielding differences, are considered (see for instance: G. Schreckenbach, T. Ziegler, *Int. J. Quantum. Chem*. **1997**, *61*, 899–918), and can thus be neglected for the purposes of this study.

[51] This value has been obtained by compressing and elongating the optimized Ru–I bonds by $\Delta r = 5$ pm each, leaving all other parameters unchanged, and by a linear fit of the resulting three $[r,\sigma(r)]$ data points. The Ru nucleus becomes deshielded with increasing Ru–I bond lengths.

[52] *The Principles of Nuclear Magnetism* (Ed.: A. Abragam), Oxford University Press, Oxford, **1961**, Chapter 9, p. 314.

[53] See for example: a) L. Hemmingsen, U. Ryde, *J. Phys. Chem*. **1996**, *100*, 4803–4809; b) V. Kellö, A. Sadlej, P. Pyykkö, D. Sundholm, M. Tokman, *Chem. Phys. Lett*. **1999**, *304*, 414–422; c) M. Gee, R. E. Wasylishen, in *Modeling NMR Chemical Shifts* (Eds.: J. C. Facelli, A. D. deDios), *ACS Symp. Ser.* **1999**, *732*, 259–276.

[54] See for instance: a) M. Pernpointer, P. Schwerdtfeger, B. A. Hess, *Int. J. Quantum Chem.* **2000**, *76*, 371–384; b) V. Kellö, A. J. Sadlej, *Phys. Rev. A* **1999**, *60*, 3575–3585; c) V. Kellö, P. Pyykkö, A. J. Sadlej, P. Schwerdtfeger, J. Thyssen, *Chem. Phys. Lett.* **2000**, *318*, 222–231, and references cited therein.

[55] M. A. Fedotov, O. L. Malkina, V. G. Malkin, *Chem. Phys. Lett*. **1996**, *258*, 330–335.

[56] Compounds **15**, **16**: M. P. Aarndts,D. J. Stufkens, A. Oskam, J. Fraanje, K. Goubitz, *Inorg. Chim. Acta*, **1997**, *256*, 93–105.

[57] Incidentally, **1** has also the largest chemical-shift anisotropy, $\Delta\sigma \approx$ 4500; there is, however, no correlation between q_{zz} and $\Delta\sigma$ for the whole set of compounds.

[58] Since no linewidth was reported in ref. [30b], we have remeasured the ^{99}Ru NMR spectrum of **6** in chloroform solution at 313 K on a 300 MHz Bruker DRX-300 spectrometer employing a 10 mm low-frequency broad-band probe (^{103}Rh – ^{91}Zr{^{1}H}; 9 MHz – 29 MHz), against a saturated reference solution of **2** in D_2O at room temperature (cf. ref. [30a]).

[59] Taken from: F. E. Wagner, U. Wagner, in *Mössbauer Isomer Shifts* (Eds.: G. K. Shenoy, F. E. Wagner), North Holland, Amsterdam, **1978**, pp. 431 – 514.

[60] R. Greatrex, N. N. Greenwood, P. Kaspi, *J. Chem. Soc. A* **1971**, 1873 – 1877 (see the appendix for an excellent discussion).

[61] The following values were employed in the conversion: $h\nu_0 = 89.4$ keV (ref. [59]), $Q_{3/2} = 2.94\,Q_{5/2}$ (T. C. Gibb, R. Greatrex, N. N. Greenwood, D. C. Puxley, K. G. Snowdon, *Chem. Phys. Lett.* **1973**, *20*, 130 – 132), and $Q_{5/2} = 7.9$ fm^2 (*CRC Handbook of Chemistry and Physics, 72nd ed.*, CRC, Boca Raton, **1991**).

[62] In addition to possible shortcomings inherent to the DFT method employed, errors may be introduced by neglect of relativistic effects (which, apparently, amount to just a few percent for nuclei from the 5th period, cf. ref. [54]) and by uncertainties in the experimental nuclear quadrupole moments (see for instance P. Pyykkö, *Z. Naturforsch* **1992**, *47a*, 189 – 196).

[63] For $[RuO_4]^-$ (**17**), D_{2d} minimum at UBP86/ECP1: Ru–O 1.758 Å, O-Ru-O 113.2°; X-ray of $KRuO_4$: 1.79 Å and 116.0° (M. D. Silverman, H. A. Levy, *J. Am. Chem. Soc.* **1954**, *76*, 3317 – 3319); $[RuCl_4N]^-$ (**18**), C_{4v} minimum: Ru–N 1.614 Å, Ru–Cl 2.360 Å, N-Ru-Cl 105.0°; X-ray of $(Ph_4As)[RuCl_4N]$: 1.570(7) Å, 2.310(1) Å, and 104.58(4)° (F. L. Phillips, A. C. Skapski, *Acta Crystallogr.* **1975**, *B31*, 2667 – 2670).

Received: January 13, 2000 [F2237]

 © WILEY-VCH Verlag GmbH, D-69451 Weinheim, 2000 0947-6539/00/0617-3280 $ 17.50+.50/0